Biosensors and Bioelectronics 25 (2009) 883–888

Contents lists available at ScienceDirect

Biosensors and Bioelectronics

journal homepage: www.elsevier.com/locate/bios

Original research paper

Direct electrochemistry of glucose oxidase and biosensing for glucose based on carbon nanotubes@SnO_2-Au composite

Fenghua Li[a], Jixia Song[a], Fei Li[a], Xiaodan Wang[a], Qixian Zhang[a], Dongxue Han[a,b], Ari Ivaska[b], Li Niu[a,b,*]

[a] State Key Laboratory of Electroanalytical Chemistry, Changchun Institute of Applied Chemistry, and Graduate University of the Chinese Academy of Sciences, Chinese Academy of Sciences, Changchun 130022, PR China
[b] Laboratory of Analytical Chemistry, Process Chemistry Centre, Åbo Akademi University, Åbo-Turku, FI-20500, Finland

ARTICLE INFO

Article history:
Received 4 June 2009
Received in revised form 30 August 2009
Accepted 31 August 2009
Available online 3 September 2009

Keywords:
Multi-walled carbon nanotubes
Tin dioxide
Ionic liquids
Au nanoparticles
Electrocatalysis
Biosensors

ABSTRACT

Multiwalled carbon nanotubes@SnO_2-Au (MWCNTs@SnO_2-Au) composite was synthesized by a chemical route. The structure and composition of the MWCNTs@SnO_2-Au composite were confirmed by means of transmission electron microscopy, X-ray photoelectron and Raman spectroscopy. Due to the good electrocatalytic property of MWCNTs@SnO_2-Au composite, a glucose biosensor was constructed by absorbing glucose oxidase (GOD) on the hybrid material. A direct electron transfer process is observed at the MWCNTs@SnO_2-Au/GOD-modified glassy carbon electrode. The glucose biosensor has a linear range from 4.0 to 24.0 mM, which is suitable for glucose determination by real samples. It should be worthwhile noting that, from 4.0 to 12.0 mM, the cathodic peak currents of the biosensor decrease linearly with increasing the glucose concentrations in human blood. Meanwhile, the resulting biosensor can also prevent the effects of interfering species. Moreover, the biosensor exhibits satisfying reproducibility, good operational stability and storage stability. Therefore, the MWCNTs@SnO_2-Au/GOD biocomposite could be promisingly applied to determine blood sugar concentration in the practical clinical analysis.

1. Introduction

The measurement of glucose concentration in blood is critical for diagnosis of diabetes mellitus. It affected approximately 171 million individuals worldwide in the year 2000 and the population is estimated to reach 366 million by the year 2030 (Wild et al., 2004). Since the first reported electrochemical glucose biosensor was developed in 1962 by Clark and Lyons (Clark and Lyons, 1962), many outstanding works have been achieved in the design and application of glucose biosensors (Heller and Feldman, 2008). In an electrochemical method, glucose oxidase (GOD) is generally used to catalyze the oxidation of glucose by oxygen to produce gluconic acid and hydrogen peroxide. The glucose in samples can be determined through amperometric monitoring of the liberated hydrogen peroxide (Moreno-Bondi et al., 1990). Therefore, the electrode materials must achieve a high electron transfer between biomolecules and electrode surface and maintain the configuration of GOD keeping the enzyme activity.

Carbon nanotubes have been considered as one of the most popular electrode materials in facilitating the direct electron transfer (DET) between the enzyme redox center and the electrode. Currently, a broad variety of reagents has been introduced to hybridize with multiwalled carbon nanotubes (MWCNTs) to form biomaterials, like metal oxides (Bao et al., 2008), quantum dots (Liu et al., 2007), metal particles (Kang et al., 2007; Luo et al., 2006; Tang et al., 2004; Zou et al., 2008), silanes (Luong et al., 2004), ionic liquids (Jia et al., 2008; Li et al., 2009a; Zhang et al., 2007), polymers (Jia et al., 2008; Li et al., 2009a), etc. In particular, metal oxide particles such as titanium oxide (Bao et al., 2008; Li et al., 2001a,b; Topoglidis et al., 2006), manganese oxide (Lvov et al., 2000), iron oxide (Zhao et al., 2006), nickel oxide (Salimi et al., 2007), zirconium oxide (Zhao et al., 2005) and tungsten oxide (Feng et al., 2006) have been used successfully for immobilizing enzymes and proteins to fabricate biosensor.

Over the last decade, Au nanoparticles (AuNPs) have attracted increasing research attention for applications in catalysis and sensors (Daniel and Astruc, 2004; Raguse et al., 2007). AuNPs generally possess excellent catalytic activity and offer a hospitable environment for biomolecules. They enable direct electrochemistry of GOD (Li et al., 2007), hemoglobin (Yang et al., 2007) and cytochrome c (Wang and Wang, 2004). In most biological applications, AuNPs should easily dissolve in aqueous solution and not aggregate (Tatumi and Fujihara, 2005). AuNPs stabilized by ionic liquid can meet the above requirements, and the resulting product has a high eletrocatalytic activity as well as long-term stability (Shan et al., 2008; Wang et al., 2008c).

* Corresponding author. Tel.: +86 431 8526 2425; fax: +86 431 8526 2800.
E-mail address: lniu@ciac.jl.cn (L. Niu).

0956-5663/$ – see front matter © 2009 Elsevier B.V. All rights reserved.
doi:10.1016/j.bios.2009.08.044

Tin oxide has generally applied in the field of sensors, electrode materials and solar cells, due to its low cost, chemical stability, useful electrical properties (Gubbala et al., 2008; Wang et al., 2008a; Wen et al., 2007). A problem worthy to be pointed out is that GOD was immobilized on tin oxide thin film to fabricate a glucose sensor (Ansari et al., 2008). However, the nanostructured SnO_2 thin film were grown at relatively high temperatures (350–450 °C) using plasma enhanced chemical vapor deposition.

In this work, SnO_2 was wrapped on MWCNTs at 60 °C by $SnCl_2$ hydrolysis in acidic solution. AuNPs were in situ dispersed over the amorphous SnO_2-wrapped MWCNTs to form MWCNTs@SnO_2-Au nanocables. Transmission electron microscopy (TEM) image shows that the MWCNTs@SnO_2 surface is covered with AuNPs at high density. The MWCNTs@SnO_2-Au composite was deposited on a glassy carbon electrode (GCE), and then a glucose biosensor was constructed by absorbing GOD on the hybrid material. The DET of GOD is observed at the MWCNTs@SnO_2-Au/GOD-modified GCE. A linear range from 4.0 to 24.0 mM was mainly studied in phosphate buffer solution (PBS), which is suitable for glucose determination by real samples. Moreover, the glucose concentration in human blood was preliminarily studied by the resulting biosensor.

2. Experimental

2.1. Reagents

MWCNTs were purchased from Shenzhen Nanotech Port Ltd. Co. (China). 1-methylimidazole (≥98%, Linhai Kaile Chemicals, China) was first distilled at reduced pressure and then used. Morphine hydrochloride was supplied by the Institute of Forensic Science, Ministry of Public Security (China). $HAuCl_4{\cdot}4H_2O$ (≥99.9%, Shanghai Chemicals, China), 3-bromopropylamine hydrobromide (98%, Aldrich), GOD (100,000–250,000 units/g, Sigma), Nafion® 117 solution (Fluka, ~5% in a mixture of aliphatic alcohols and water), ascorbic acid (AA, ≥99.0%, Fluka), dopamine hydrochloride (DA, Aldrich), uric acid (UA, Aldrich), H_2O_2 (30%, Beijing Chemicals, China), KH_2PO_4 (≥99.5%, Beijing Chemicals, China), $Na_2HPO_4{\cdot}12H_2O$(≥99.0%, Laiyang Chemicals, China), ethanol (99.8%, Beijing Chemicals, China), ethyl acetate (99.7%, Beijing Chemicals, China), HCl (36–38%, Beijing Chemicals, China), HNO_3 (65%, Beijing Chemicals, China), H_2SO_4 (98%, Beijing Chemicals, China), $SnCl_2{\cdot}2H_2O$ (98.0%, Beijing Chemicals, China) and urea (99.0%, Beijing Chemicals, China) were used as received. All aqueous solutions were prepared with ultrapure water (>18 MΩ cm) that was obtained from a Milli-Q Plus system (Millipore).

2.2. Synthesis of amine-terminated ionic liquid (IL-NH_2)

IL-NH_2 was prepared following our previous report (Zhang et al., 2006). Briefly, 1.10 g 3-bromopropylamine hydrobromide and 0.40 mL 1-methylimidazole were added to 12.5 mL ethanol. And then the resulting colourless solution was refluxed under nitrogen for 24 h. Finally, the turbid mixture was purified by recrystallization and the white product was then dried for 24 h at 60 °C under vacuum.

2.3. Preparation of MWCNTs@SnO_2-Au composite

The as-received MWCNTs were treated with HNO_3 at 60 °C for 12 h by continuous stirring. The product was centrifuged and washed with ultrapure water until its pH value approaches to 7. The MWCNTs@SnO_2 nanocables were prepared according to the method reported by Chen et al. (Chen et al., 2008). Briefly, 30 mg of MWCNTs were dissolved in 18 mL of water at room temperature. Subsequently, 0.15 mL of HCl, 0.66 g of $SnCl_2{\cdot}2H_2O$, and 0.3 g of urea were added. The mixture was then continually stirred at 60 °C for 6 h. The product was rinsed with distilled water and then dried at 60 °C under vacuum. For the preparation of MWCNTs@SnO_2-Au composite, 1.0 mg of MWCNTs@SnO_2 and 0.10 g of IL-NH_2 were dissolved in 5.2 mL of water, and then 0.74 mL of 13.5 mM $HAuCl_4$ aqueous solution was added dropwise over several minutes. After stirring for 12 h, the product was centrifuged, washed with ultrapure water and then dried at room temperature under vacuum.

2.4. Preparation of MWCNTs@SnO_2-Au and MWCNTs@SnO_2-Au/GOD composite films

The GCE (3 mm in diameter) was polished subsequently with 1.0, 0.3 and 0.05 μm alumina slurry, and sonicated in water for several times. To prepare the MWCNTs@SnO_2-Au-modified GCE, 3 μL of 2 mg/mL MWCNTs@SnO_2-Au aqueous solution were coated on the polished GCE with a microsyringe and dried in air. In order to prepare MWCNTs@SnO_2-Au/GOD composite film, 5 μL of 3 mg/mL GOD PBS were dropped on the MWCNTs@SnO_2-Au-modified GCE, and then dried for ca. 24 h at 4 °C. The illustration of our assembly electrode was shown in Fig. S.1. After polishing, the MWCNTs@SnO_2-Au/GOD-modified assembly electrode was prepared in the same way as the MWCNTs@SnO_2-Au/GOD-modified GCE. Finally, 2 μL of 0.5% Nafion aqueous solution was dropped on the MWCNTs@SnO_2-Au/GOD composite film to prevent the loss of biocomposite. Those enzyme-modified electrodes were stored at 4 °C in refrigerator when they were not in use.

2.5. Instruments and measurements

TEM image was taken with JEOL 2000 transmission electron microscope operating at 200 kV. X-ray photoelectron spectroscopy (XPS) analysis was carried out on an ESCALAB MK II X-ray photoelectron spectrometer. Raman spectra were collected using a Renishaw Raman system model 1000 spectrometer. The 514.5-nm radiation from a 20 mW air-cooled argon ion laser was used as exciting source. Cyclic voltammetry (CV) scans were performed using a CHI660 electrochemical workstation (CHI, USA). All electrochemical measurements (besides blood sample test) were performed in a three-electrode electrochemical cell. A Pt wire and a KCl-saturated Ag/AgCl electrode were used as the counter and reference electrode, respectively. The assembly electrode consists of a GCE (as working electrode, 1 mm in diameter), an Ag sheet (as reference electrode) and a Pt sheet (as counter electrode).

3. Results and discussion

3.1. Structure characterization

Fig. 1A and B display the TEM images of MWCNTs@SnO_2 and MWCNTs@SnO_2-Au nanocables, respectively. From the TEM image of MWCNTs@SnO_2, we can see that there is a uniform layer coating the MWCNTs. The diameter of these nanocables is about 20–35 nm, and the thickness of the coating layer is about 5–12 nm. After immobilization of AuNPs, the resulting TEM image reveals that spherical Au particles are present as dark dots with non-ordered distribution (Fig. 1B). The diameter of Au nanoparticles ranges from 3.4 to 6.0 nm, and their mean diameter is 4.5 nm (inset of Fig. 1B).

The XPS spectrum of MWCNTs@SnO_2-Au composite is shown in Fig. S.2. The peaks of Sn $3d_{5/2}$ and Sn $3d_{3/2}$ for the amorphous SnO_2 (top-left inset of Fig. S.2) are found at 487.8 eV and 496.3 eV, respectively, in well agreement with results reported by the previous literature (Li et al., 2008). It is further confirmed that the SnO_2 coating layer was wrapped on the MWCNTs walls. The Au $4f_{7/2}$ and Au $4f_{5/2}$ peaks due to the deposited AuNPs reduced by IL-NH_2 (Wang et al., 2008c) appear at ca. 83.9 and 87.7 eV, respectively.

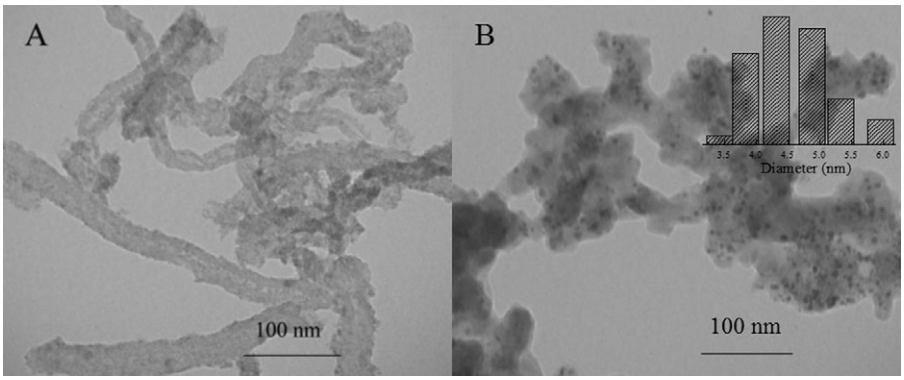

Fig. 1. TEM images of (A) the MWCNTs@SnO_2 and (B) the MWCNTs@SnO_2-Au nanocables, particle size distribution as inset.

Fig. S.3 shows the Raman spectra of the MWCNT-COOH, MWCNTs@SnO_2 and MWCNTs@SnO_2-Au nanocomposite. The characteristic peaks of MWCNTs are observed at 1352 cm^{-1} (D band) and 1584 cm^{-1} (G band), respectively (Wang et al., 2008b). The ratio of the D band to the G band (*R* value) is from 1.05 to 1.22, associated with the change from MWCNT-COOH to MWCNTs@SnO_2. It is suggested that SnO_2 particles have improved the roughness of MWCNTs (Chen et al., 2008). The *R* value of MWCNTs@SnO_2-Au nanocomposite is reduced to 1.11, which indicates that AuNPs grew in the pores of SnO_2 and some defects disappeared. From the MWCNTs@SnO_2 to the MWCNTs@SnO_2-Au composite, the reduction of the *R* value and the little upshift in the two bands might be related to the interactions between MWCNTs@SnO_2 and deposited Au atoms (Zhang and Wang, 2007).

3.2. Electrocatalytical properties

Fig. 2A displays the CVs at MWCNTs@SnO_2-Au in N_2-saturated and O_2-saturated 0.05 M PBS (pH 7.0) solution. An obvious reduction wave of O_2 at MWCNTs@SnO_2-Au-modified GCE is observed at ca. −0.25 V (solid black curve). In contrast, the reduction potential of O_2 at a bare GCE is at ca. −0.55 V (solid gray curve). However, no peaks are seen in the N_2-saturated solution at the above two electrodes. Therefore, we conclude that MWCNTs@SnO_2-Au retains a high electrocatalytical activity toward the reduction of O_2. The electrocatalytical effect of H_2O_2 is also observed at the same electrode (Fig. 2B). The initial potential of H_2O_2 reduction is about −0.03 V at the MWCNTs@SnO_2-Au-modified GCE (solid black curve). Therefore, these results clearly suggest that the MWCNTs@SnO_2-Au composite can electrocatalytically reduce O_2 and H_2O_2, which is in favor of further utilization of glucose sensing.

3.3. Biocompatibility and glucose biosensing

Fig. 3A shows the CV curve at the MWCNTs@SnO_2-Au/GOD-modified GCE in 0.05 M N_2-saturated PBS (solid curve). A pair of well-defined and nearly symmetric redox peaks is observed. The peak-to-peak separation (ΔEp) is calculated to be ca. 0.035 V and the ratio of the cathodic current over the anodic one is close to 1. For comparison, the CV curve without GOD at MWCNTs@SnO_2-Au-modified GCE does not show such redox waves (dashed curve). It indicates that the redox waves are ascribed to the redox active center in GOD biomolecules (Liu et al., 2005) and the DET of GOD can be achieved on the MWCNTs@SnO_2-Au-modified GCE. Fig. 3B shows CVs of the MWCNTs@SnO_2-Au/GOD-modified GCE at various scan rates. The small ΔEp value and the linear relationship ($R = 0.999$) between the peak currents and scan rates indicate that the redox process of the prepared biocomposite is a reversible and surface-confined process. Therefore, the MWCNTs@SnO_2-Au composite might facilitate a reversible electron transfer process between GOD and electrode substrate.

MWCNTs were pointed out to play an important role in the DET of GOD (Deng et al., 2008). Meanwhile, SnO_2 as linking material can provide a well conductive and porous substrate to facilitate the reversible electron transfer and immobilize GOD molecules in the pores (Ansari et al., 2008; Feng et al., 2006; Li et al., 2001b). In addition, hydroxyl groups on SnO_2 can absorb IL-NH_2 on MWCNTs@SnO_2 through electrostatic interaction. IL-NH_2 might play an additionally delicate role in the effective immobilization of GOD on MWCNTs@SnO_2 through ionic interaction. As known, GOD

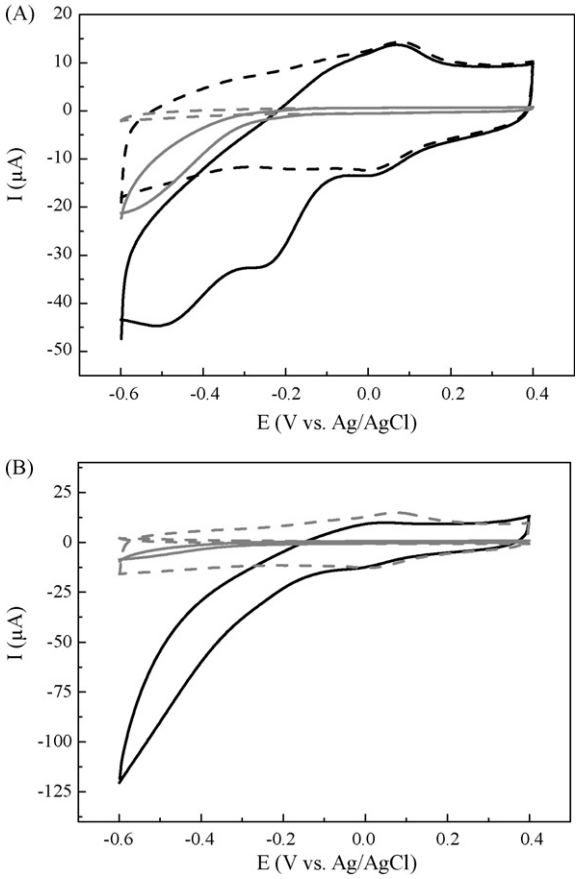

Fig. 2. (A) CV curves at the bare GCE (gray) and the MWCNTs@SnO_2-Au-modified GCE (black) in 0.05 M O_2-saturated (solid) and N_2-saturated (dashed) PBS (pH 7.0) solution. (B) CV curves at the bare GCE (gray) and the MWCNTs@SnO_2-Au-modified GCE (black) in 0.05 M N_2-saturated PBS (pH 7.0) solution in the absence (dashed) and in the presence (solid) of 6.0 mM H_2O_2. Scan rate: 0.05 Vs^{-1}.

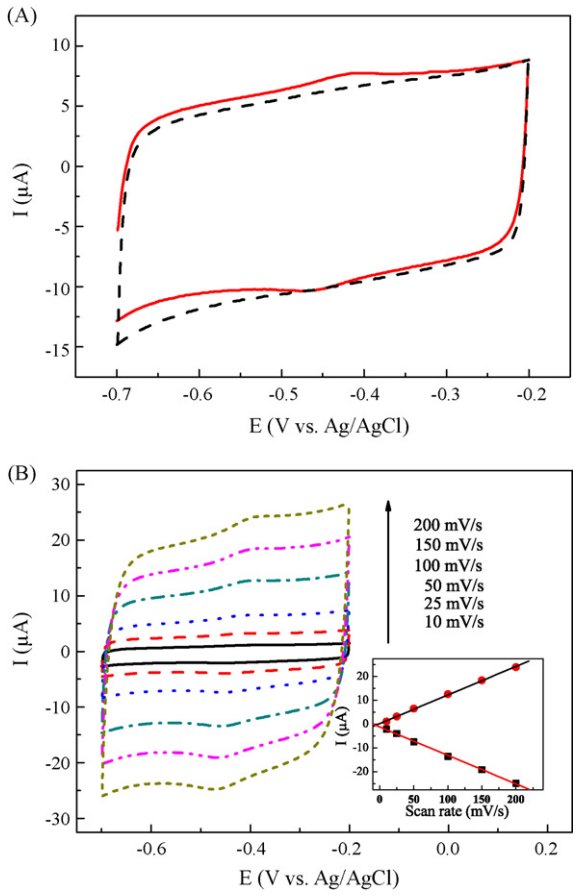

Fig. 3. CV grams (A) at the MWCNTs@SnO_2-Au-modified (dashed), MWCNTs@SnO_2-Au/GOD-modified GCE (solid) in 0.05 M N_2-saturated PBS (pH 7.0) at a scan rate of 0.05 Vs^{-1}, (B) at the MWCNTs@SnO_2-Au/GOD-modified GCE in 0.05 M N_2-saturated PBS solution at various scan rates. Scan rate: 10, 25, 50, 150 and 200 mVs^{-1} from inner to outer. Inset is the calibrated plot of peak currents vs. scan rates.

is net negatively charged in the pH 7.0 solution, in contrast, the IL-like unit (imidazolium cation) is positively charged. Moreover, like many other ILs, here the charge state of IL-like unit is not depended on pH. Therefore, the positively charged IL-like unit is in favor of conjugation of negatively charged GOD (pH 7.0). Furthermore, Br^- anion in IL-NH_2 is ready to be exchanged (Zhang et al., 2006) with GOD. Finally, AuNPs have good electrocatalysis toward H_2O_2 reduction, which is generated during the course of the GOD-catalyzed oxidation of glucose in the presence of dissolved oxygen.

A glucose sensor was fabricated to verify the bioactivity of immobilized GOD deposited on the MWCNTs@SnO_2-Au composite. Fig. 4 shows the CV grams at the MWCNTs@SnO_2-Au/GOD-modified GCE in different concentrations of glucose in air-saturated PBS. The peak current decreases with the increase of the glucose concentrations (Zhang et al., 2007). It suggests that the specific enzyme-substrate activity of GOD has been reserved in the MWCNTs@SnO_2-Au composite. As shown in the inset of Fig. 4, a linear relationship between the amperometric responses and the concentrations of glucose is observed ranging from 4.0 to 24.0 mM. The detection limit of the MWCNTs@SnO_2-Au/GOD-modified GCE biosensor is 5 μM by amperometric current-time method (Fig. S.4). Therefore, the MWCNTs@SnO_2-Au composite has a great potential for the application in electrochemical detection of glucose.

As known, fasting blood glucose ≥7.0 mM (126 mg/dL) and/or postprandial blood glucose ≥11.1 mM (200 mg/dL) is the base of diagnosis of diabetes. So the linear glucose response from 4.0 to 24.0 mM based on our MWCNTs@SnO_2-Au/GOD biocomposite is suitable for determining blood glucose concentration. To perform

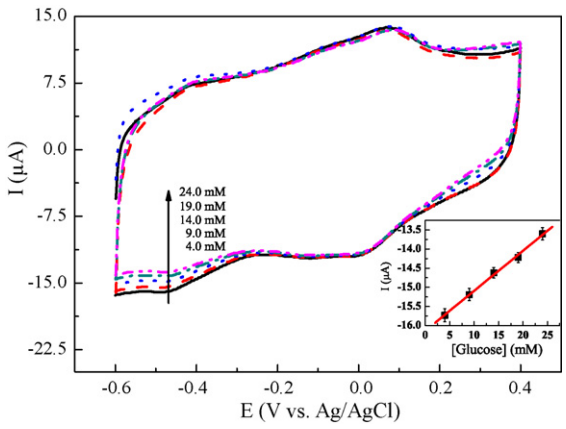

Fig. 4. CV grams at the MWCNTs@SnO_2-Au/GOD-modified GCE in various concentrations of glucose PBS (pH 7.0): 4.0, 9.0, 14.0, 19.0 and 24.0 mM from outer to inner. Inset is the calibration curve corresponding to amperometric responses. Scan rate: 0.05 Vs^{-1}.

blood sample test, 30 μL of human blood (4.0 mM sugar concentration) were coated on the MWCNTs@SnO_2-Au/GOD-modified assembly electrode with a microsyringe. The drop of blood must cover all the three electrodes of the assembly electrode, and is used as electrolyte. The cathodic current decreases with successive addition of 0.4 μL 0.17 M glucose solution (Fig. 5). From 4.0 to 12.0 mM, the amperometric responses linearly change with the glucose concentration (inset of Fig. 5).

3.4. Interference study and performance evaluation

The glucose amperometric enzyme sensors are based on the electro-reduction of hydrogen peroxide produced by the enzymatic oxidation of glucose. In general, the amperometric detection of H_2O_2 could be undertaken either by reduction or oxidation. However, within the living body, there is concomitant electro-oxidation of many interfering species, such as AA, DA, UA, alcohol and so on (Endo et al., 2009; Wang et al., 2002). Therefore, the electro-reduction method was carried out in this paper in order to remove the serious interference in the practical sample analysis. The biosensor was immersed into a cell containing 10 mL of 0.05 M air-saturated PBS (pH 7.0) with stirring and then each substrate solution was added to the cell. For the glucose solution (0.2 mM), the sensor output increases, and a maximum current is obtained within 25 s. When AA (0.2 mM), DA (0.2 mM), UA (0.2 mM), alco-

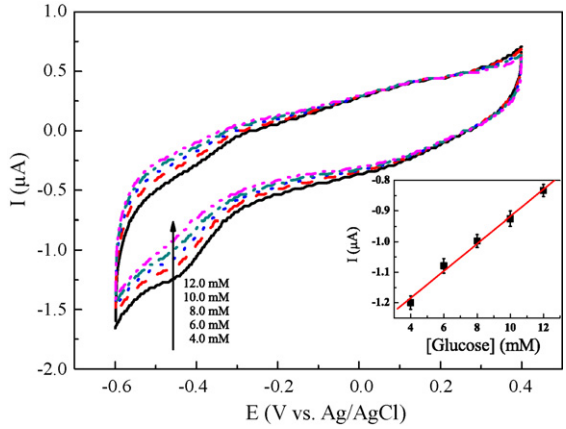

Fig. 5. CV grams at the MWCNTs@SnO_2-Au/GOD-modified assembly electrode in blood sample containing 4.0, 6.0, 8.0, 10.0, 12.0 mM glucose from outer to inner. Inset is the calibration curve corresponding to amperometric responses. Scan rate: 0.05 Vs^{-1}.

Table 1
Performance comparison of the resulting biosensor for glucose detection with other sensors.

Method	Real sample	Linear range (mM)	Precision	References
Hybrids-modified assembly electrode	Human blood	4.0–24.0 mM	2.5%	This work
Screen-printed sensor	Bovine serum	0.025–2.0 mM	3.3%	Crouch et al. (2005)
Polyvinylferrocene-Au-GOD enzyme sensor	Serum	Up to 22.5 mM	5%	Sulak et al. (2006)
Microfluidic system	Human blood	1.61–30.0 mM	14.13%	Huang et al. (2007)
Charge transfer technique glucose sensor	Human blood	0.1–25.0 mM	Within 1%	Lee et al. (2008)
Photoluminescence method	Serum	0.5–16.0 mM	10%	Li et al. (2009b)
Needle-type enzyme sensor	Fish blood	0.01–8.0 mM	1.93%	Endo et al. (2009)

hol (17 mM), and morphine (1.0 mM) solution were added to the cell, the current does not change (Fig. S.5). Therefore, the biosensor can eliminate the interference of other molecules in blood by electro-reduction method. The MWCNTs@SnO_2-Au/GOD biocomposite as a promising candidate could be used to determine blood glucose concentration in the practical clinical analysis. In addition, the influence on the specificity of substrate-enzymatic reaction is very complicated due to the existence of interfering species. We hope we will give a reasonable answer in the nearest future.

The glucose detection performances of the proposed biosensor are compared with other sensors. As shown in Table 1, the MWCNTs@SnO_2-Au/GOD-modified electrode offers reasonable linear range for glucose detection of real sample and the precision of detection is much better than the previous report of glucose detection of human blood (Huang et al., 2007). However, in comparison with the charge transfer glucose sensor previously described by Lee et al. (Lee et al., 2008), it shows little bad performance. The relative standard derivation (RSD) of our method is 2.5% for 15 detections in 6.0 mM glucose blood sample at a same modified electrode. However, the method and mechanism are totally different from the previous report which was performed on measurements of small (D-gluconate + H^+) ion fluctuation to determine the glucose concentration. In this work, the measurements of glucose are achieved via electrochemical detection of the liberated H_2O_2 during the oxidation of glucose. It is worthwhile noting that the cost of the biosensor is even lower than that of the currently used methods. Moreover, the amount of blood in one test is only 30 μL, which is acceptable for patients. Furthermore, this biosensor can be used even over 15 times. Therefore, the biosensor could be promisingly applied to determine blood glucose concentration in the practical clinical analysis. The storage stability of the biosensor was also investigated. After two week storage at 4 °C, the redox peak currents retain 89% of their initial response values. It is hopefully that the performance of our biosensor can be improved further by combining screen-printing technique.

About 3 dollars are charged for a blood glucose test at hospital. Recently, the popular method used at home is blood glucose strip. The price of blood glucose strip is about 1 dollar but the strip cannot be used repeatedly. Moreover, the reproducibility of the strip method is not satisfied. The detailed calculation of the cost of MWCNTs@SnO_2-Au/GOD biocomposite is as follows. Firstly, the cost of the assembly electrode was about 30 dollars and it can be used for several thousands times. On the assumption that one assembly electrode can be used for 1000 times, only 0.03 dollars are needed in one test at the electrode part. Secondly, the cost of the MWCNTs@SnO_2-Au composite is ca. 100 dollars/g. However, the amount of biocomposite using for one chip is 6×10^{-6} g. So the cost of the MWCNTs@SnO_2-Au composite for one chip is only ca. 6×10^{-4} dollars; Thirdly, the price of GOD is 6400 dollars/g. 1.5×10^{-5} g of GOD is needed for one chip. Thus the cost of GOD is ca. 0.1 dollars for one chip. Finally, the price of Nafion for one chip is ca. 0.002 dollars. In a word, the cost of biosensor is much less than 0.02 dollars in one test if one chip is used for 10 times. Therefore, the cost of the biosensor is less than that of the currently used methods. Combining with screen-printing technology, the cost of biosensor will be further decreased.

3.5. Stability

The DET of GOD in the biosensor exhibits high stability, and its voltammetric response remains stable even after continuous scanning for 50 cycles. The reproducibility of enzyme electrode construction was estimated from the response to 10.0 mM glucose at five-enzyme electrodes prepared under the same conditions. The results reveal that the biosensor has satisfying reproducibility with a RSD of 5.3%. The operational stability of the enzyme electrode was measured by a same enzyme electrode's continuous response to 0.05 M PBS containing 10 mM glucose. The RSD is 3.4% for continuous five-time determinations. After one-week storage at 4 °C, the response current of the biosensor decreases 2.6% in 0.05 M PBS containing 10.0 mM glucose. The redox peak currents retain 93% of their initial response values after two weeks. After one month, the redox peak currents retain 87% of their initial response. This implies that the MWCNTs@SnO_2-Au/GOD-modified electrode has good reproducibility and stability. The good representation of the biosensor can be attributed to following reasons. First, the conductive and mesoporous structure of SnO_2 facilitate to immobilize the enzyme and keep the configuration of GOD. Second, IL-NH_2 has high ionic conductivity and large quantities of amine groups that are favorable to maintain the activity of the enzyme. Moreover, the strong interaction between the negatively charged enzyme and the positively charged composite avoids the enzyme loss. Third, AuNPs offer a hospitable environment for GOD and possess satisfying electrocatalysis toward reduction of oxygen and hydrogen peroxide. Therefore, the MWCNTs@SnO_2-Au composite could be used to immobilize GOD efficiently and further retain the bioactivity of adsorbed GOD.

4. Conclusions

MWCNTs@SnO_2-Au nanocomposite was prepared by a chemical route. The biosensor based on MWCNTs@SnO_2-Au/GOD-modified GCE was prepared to detect glucose. A linear range from 4.0 to 24.0 mM was mainly studied in PBS, which is suitable for glucose determination by real samples. The glucose concentration in human blood was preliminarily studied by the hybrids modified-assembly electrode. From 4.0 to 12.0 mM, the cathodic peak currents of the biosensor decrease linearly with increasing the glucose concentrations. Several interfering species possible appearing in blood such as AA, DA, UA, alcohol and morphine, do not influence glucose determination. The cost of the biosensor is lower than that of the currently used methods. The biosensor exhibits satisfying reproducibility, good operational stability and storage stability. Therefore, the MWCNTs@SnO_2-Au/GOD biocomposite could be promisingly applied to determine blood glucose concentration in the practical clinical analysis.

Acknowledgements

The authors are most grateful to the NSFC, China (No. 20673109) and Ministry of Science and Technology (No. 2007AA03Z354 and 2007BAK26B06) for their financial support.

Appendix A. Supplementary data

Supplementary data associated with this article can be found, in the online version, at doi:10.1016/j.bios.2009.08.044.

References

Ansari, S.G., Ansari, Z.A., Wahab, R., Kim, Y.-S., Khang, G., Shin, H.-S., 2008. Biosens. Bioelectron. 23, 1838–1842.
Bao, S.-J., Li, C., Zang, J.-F., Cui, X.-Q., Qiao, Y., Guo, J., 2008. Adv. Funct. Mater. 18, 591–599.
Chen, G., Wang, Z., Xia, D., 2008. Chem. Mater. 20, 6951–6956.
Clark, L.C., Lyons Jr., C., 1962. Ann. N. Y. Acad. Sci. 102, 29–45.
Crouch, E., Cowell, D.C., Hoskins, S., Pittson, R.W., Hart, J.P., 2005. Biosens. Bioelectron. 21, 712–718.
Daniel, M.-C., Astruc, D., 2004. Chem. Rev. 104, 293–346.
Deng, C., Chen, J., Chen, X., Xiao, C., Nie, L., Yao, S., 2008. Biosens. Bioelectron. 23, 1272–1277.
Endo, H., Yonemori, Y., Hibi, K., Ren, H., Hayashi, T., Tsugawa, W., Sode, K., 2009. Biosens. Bioelectron. 24, 1417–1423.
Feng, J.-J., Xu, J.-J., Chen, H.-Y., 2006. Electrochem. Commun. 8, 77–82.
Gubbala, S., Chakrapani, V., Kumar, V., Sunkara, M.K., 2008. Adv. Funct. Mater. 18, 2411–2418.
Heller, A., Feldman, B., 2008. Chem. Rev. 108, 2482–2505.
Huang, C.-J., Chen, Y.-H., Wang, C.-H., Chou, T.-C., Lee, G.-B., 2007. Sensor. Actuat. B 122, 461–468.
Jia, F., Shan, C., Li, F., Niu, L., 2008. Biosens. Bioelectron. 24, 945–950.
Kang, X., Mai, Z., Zou, X., Cai, P., Mo, J., 2007. Anal. Biochem. 369, 71–79.
Lee, S.-R., Sawada, K., Takao, H., Ishida, M., 2008. Biosens. Bioelectron. 24, 650–656.
Li, F., Wang, Z., Shan, C., Song, J., Han, D., Niu, L., 2009a. Biosens. Bioelectron. 24, 1765–1770.
Li, J., Yu, J., Zhao, F., Zeng, B., 2007. Anal. Chim. Acta. 587, 33–40.
Li, L.-L., Zhang, W.-M., Yuan, Q., Li, Z.-X., Fang, C.-J., Sun, L.-D., Wan, L.-J., Yan, C.-H., 2008. Cryst. Growth. Des. 8, 4165–4172.
Li, Q., Luo, G., Feng, J., 2001a. Electroanalysis 13, 359–363.
Li, Q., Luo, G., Feng, J., Zhou, Q., Zhang, L., Zhu, Y., 2001b. Electroanalysis 13, 413–416.
Li, X., Zhou, Y., Zheng, Z., Yue, X., Dai, Z., Liu, S., Tang, Z., 2009b. Langmuir 25, 6580–6586.
Liu, Q., Lu, X., Li, J., Yao, X., Li, J., 2007. Biosens. Bioelectron. 22, 3203–3209.
Liu, Y., Wang, M., Zhao, F., Xu, Z., Dong, S., 2005. Biosens. Bioelectron. 21, 984–988.
Luo, X., Killard, A.J., Smyth, M.R., 2006. Electroanalysis 18, 1131–1134.
Luong, J.H.T., Hrapovic, S., Wang, D., Bensebaa, F., Simard, B., 2004. Electroanalysis 16, 132–139.
Lvov, Y., Munge, B., Giraldo, O., Ichinose, I., Suib, S.L., Rusling, J.F., 2000. Langmuir 16, 8850–8857.
Moreno-Bondi, M.C., Wolfbeis, O.S., Leiner, M.J.P., Schaffar, B.P.H., 1990. Anal. Chem. 62, 2377–2380.
Raguse, B., Chow, E., Barton, C.S., Wieczorek, L., 2007. Anal. Chem. 79, 7333–7339.
Salimi, A., Sharifi, E., Noorbakhsh, A., Soltanian, S., 2007. Biosens. Bioelectron. 22, 3146–3153.
Shan, C., Li, F., Yuan, F., Yang, G., Niu, L., Zhang, Q., 2008. Nanotechnology 19, 285601 (6 pp).
Sulak, M.T., Gökdoğan, Ö., Gülce, A., Gülce, H., 2006. Biosens. Bioelectron. 21, 1719–1726.
Tang, H., Chen, J., Yao, S., Nie, L., Deng, G., Kuang, Y., 2004. Anal. Biochem. 331, 89–97.
Tatumi, R., Fujihara, H., 2005. Chem. Commun., 83–85.
Topoglidis, E., Campbell, C.J., Cass, A.E.G., Durrant, J.R., 2006. Electroanalysis 18, 882–887.
Wang, L., Wang, E., 2004. Electrochem. Commun. 6, 49–54.
Wang, Y.D., Djerdj, I., Antonietti, M., Smarsly, B., 2008a. Small 4, 1656–1660.
Wang, Z., Zhang, Q., Kuehner, D., Xu, X., Ivaska, A., Niu, L., 2008b. Carbon 46, 1687–1692.
Wang, Z., Zhang, Y., Zhang, Q., Shen, Y., Kuehner, D., Ivaska, A., Niu, L., 2008c. Green Chem. 10, 907–909.
Wang, Z., Liu, J., Liang, Q., Wang, Y., Luo, G., 2002. Analyst 127, 653–658.
Wen, Z., Wang, Q., Zhang, Q., Li, J., 2007. Adv. Funct. Mater. 17, 2772–2778.
Wild, S., Roglic, G., Green, A., Sicree, R., King, H., 2004. Diabetes Care 27, 1047–1053.
Yang, M., Qu, F., Li, Y., He, Y., Shen, G., Yu, R., 2007. Biosens. Bioelectron. 23, 414–420.
Zhang, R., Wang, X., 2007. Chem. Mater. 19, 976–978.
Zhang, Y., Shen, Y., Han, D., Wang, Z., Song, J., Li, F., Niu, L., 2007. Biosens. Bioelectron. 23, 438–443.
Zhang, Y., Shen, Y., Yuan, J., Han, D., Wang, Z., Zhang, Q., Niu, L., 2006. Angew. Chem. Int. Ed. 45, 5867–5870.
Zhao, G., Feng, J.-J., Xu, J.-J., Chen, H.-Y., 2005. Electrochem. Commun. 7, 724–729.
Zhao, G., Xu, J.-J., Chen, H.-Y., 2006. Electrochem. Commun. 8, 148–154.
Zou, Y., Xiang, C., Sun, L.-X., Xu, F., 2008. Biosens. Bioelectron. 23, 1010–1016.